Notes

Contribution from The Max-Planck-Institut
für Festkörperforschung, Heisenbergstrasse 1,
D-7000 Stuttgart 80, Federal Republic of Germany

Chemical Intercalation of Sodium into α-Nb_3Cl_8

J. R. Kennedy*,[1] and A. Simon*

Received August 14, 1990

Introduction

Only recently have the binary metal halides been shown to offer an intercalation chemistry (with the exception of hydrogen[2]), yet the three examples known cover a range of structure types ($RuBr_3$, 1D chain structure;[3] α-$RuCl_3$, 2D layer structure;[3] Nb_6I_{11}, 3D cluster structure[4]). We report here the synthesis of β'-$NaNb_3Cl_8$, the first characterized example of an unsolvated alkali-metal-intercalated binary metal halide, from a room-temperature heterogeneous reaction of the layered polymeric cluster compound α-Nb_3Cl_8 with a THF solution of $(Na^+)_2bzph^{2-}$ and the subsequent deintercalation of β'-$NaNb_3Cl_8$ to α-Nb_3Cl_8 by reaction with water or methanol. The results offer a unique opportunity to discuss the influence of the halide–halide and halide–metal orbital interactions in determining the stability of closely related structures.

The α-structure of Nb_3Cl_8 is closely related to several other layered structure types all constructed from interconnected M_3X_{13} [X = Cl, Br, I (M = Nb); X = O (Mo, W)] cluster units through shared anions ($M_3X_{13} \rightarrow M_3X_4X_{6/2}X_{3/3} = M_3X_8$).[5] M_3X_8 represents one X–M–X cluster layer, and the structure type is determined from the orientation of each M_3X_8 cluster layer relative to its stacking neighbors. Of concern here are five structure types that shall be denoted as the α-type (α-Nb_3Cl_8),[6] β-type (β-Nb_3Br_8, β-Nb_3I_8),[5a] β'-type ($LiZn_2Mo_3O_8$, $Zn_3Mo_3O_8$),[5b,7] α'-type (unknown for M_3X_8), and γ-type (unknown for M_3X_8), which all possess a crystallographic inversion center. There are two nonequivalent van der Waals gaps in any two M_3X_8 layered series. One of these gaps, the A-gap, is formed from terminal μ_2 intercluster-bridging (X1)[8] and face-capping (X4) anions, and the second gap, the B-gap, is formed from edge-bridging (X2) and terminal μ_3 intercluster-bridging (X3) anions (Figure 1a). The α- and α'-forms are both 2T (Ramsdell notation)[9] structures in $P\bar{3}m1$, where the former has an h-anion lattice (Jagodzinski notation)[10] and the latter a non-close-packed AABC anion lattice. The β'-, β-, and γ-types are 6R structures in $R\bar{3}m$, with the β- and γ-types having a cchh- and the β'-type a c-anion lattice. Parts b–f of Figure 1 illustrate the structural relationships between the five types.

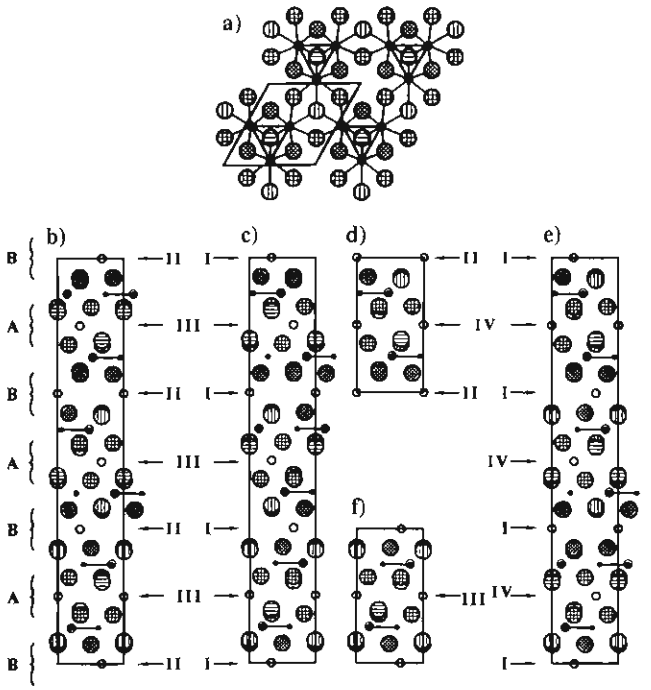

Figure 1. (a) Representation of one M_3X_8 cluster layer as viewed down the *c* axis. (b–f) Structural relationships of the layer stacking sequences: (b) γ-type; (c) β'-type; (d) α-type; (e) β-type; (f) α'-type. Type of gap and sodium site (refer to Figure 3) are illustrated. The orientations of the cells have been chosen to highlight the relationships. The Nb_3 triangles are projected down an edge. Key: Nb, solid filled circles; X1, checkered circles; X2, hatched circles; X3, vertically striped circles; X4, horizontally striped circles; Na, empty circles.

Experimental Section

α-Nb_3Cl_8 was prepared and purified by literature methods.[11] Benzophenone (bzph) was purchased and dried under vacuum (10^{-6} Torr) for several days. Tetrahydrofuran (THF) was dried and distilled twice under argon atmosphere from sodium/benzophenone immediately prior to use. All glassware was flame-dried under vacuum. All operations were carried out under argon atmosphere by using standard techniques for handling air-sensitive compounds[12] unless otherwise stated.

Preparation. A 130-mg (0.73-mmol) sample of bzph was added with an excess (50 mg) of freshly cut Na to a 100-mL Schlenk flask with a magnetic stir bar in an argon-atmosphere drybox. Onto this composition was then distilled ~35 mL of THF solvent, and the mixture was allowed to stir for ~20 h, after which time the solution was a deep red/violet color, indicative of $(Na^+)_2bzph^{2-}$ formation. This solution was then decanted into an addition funnel, which was connected to a 100-mL Schlenk flask charged with 312 mg (0.555 mmol) of crystalline α-Nb_3Cl_8. The flask was cooled to ~−75 °C with an ethanol/dry ice bath and the $(Na^+)_2bzph^{2-}$/THF solution added dropwise over a period of ~20 min. The reaction mixture was allowed to warm to room temperature over a 1–2-h period, during which time the solution over the α-Nb_3Cl_8 remained a rich red/violet color. Over the next ~10 h, at room temperature, the solution turned to a blue/green color, indicative of reaction and Na^+bzph^- formation. The solution remained this color for the next ~12 h. At this point the reaction mixture was filtered, washed three times each with fresh THF (syringe technique), and dried in vacuo for ~24 h. The solid crystalline product mixture was then returned to the drybox, where samples were separated for X-ray investigation and wet chemical analysis. The product appears black with a deep red luster. Chemical analysis on two samples gave compositions of $Na_{0.719}Nb_3Cl_8$ and

(1) Alexander von Humboldt Fellowship, 1987–1989.
(2) For example: Corbett, J. D. Intercalation of Halides. In *Intercalation Chemistry*; Whittingham, M. S., Jacobson, A. J., Eds.; Academic Press: New York, 1982; pp 361–374.
(3) (a) Schöllhorn, R.; Steffen, R.; Wagner, K. *Angew. Chem.* **1983**, *95*, 559. (b) Steffen, R.; Schöllhorn, R. *Solid State Ionics* **1986**, *22*, 31.
(4) Kennedy, J. R.; Simon, A. To be published.
(5) For various representations and descriptions see: (a) Simon, A.; von Schnering, H.-G. J. *Less-Common Met.* **1966**, *11*, 31. (b) Torardi, C. C.; McCarley, R. E. *Inorg. Chem.* **1985**, *24*, 476. (c) Hulliger, F. In *Structural Chemistry of Layered-Type Phases*; Levy, F., ed.; D. Reidel: Dordrecht, Holland, 1976. (d) Schäfer, H.; Schnering, H.-G. *Angew. Chem.* **1964**, *76*, 833. (e) Kepert, D. L.; Marshall, R. E. *J. Less-Common Met.* **1974**, *34*, 153. (f) Ansell, G. B.; Katz, L. *Acta Crystallogr.* **1966**, *21*, 482.
(6) von Schnering, H.-G.; Wöhrle, H.; Schäfer, H. *Naturwissenschaften* **1961**, *48*, 159. See also ref 5c, p 319.
(7) McCarley, R. E. *Philos. Trans. R. Soc. London, A* **1982**, *308*, 141.
(8) Atom-numbering scheme follows that found in refs 5b and 7.
(9) Ramsdell, L. S. *Am. Miner.* **1947**, *32*, 64.
(10) Pearson, W. B. *The Crystal Chemistry and Physics of Metals and Alloys*; Wiley-Interscience: New York, London, Sydney, Toronto, 1972.
(11) Schäfer, H.; Dohmann, K.-D. Z. *Anorg. Allg. Chem.* **1959**, *300*, 1. See also ref 6.
(12) Shriver, D. F. *The Manipulation of Air Sensitive Compounds*; McGraw-Hill: New York, 1969.

0020-1669/91/1330-2564$02.50/0

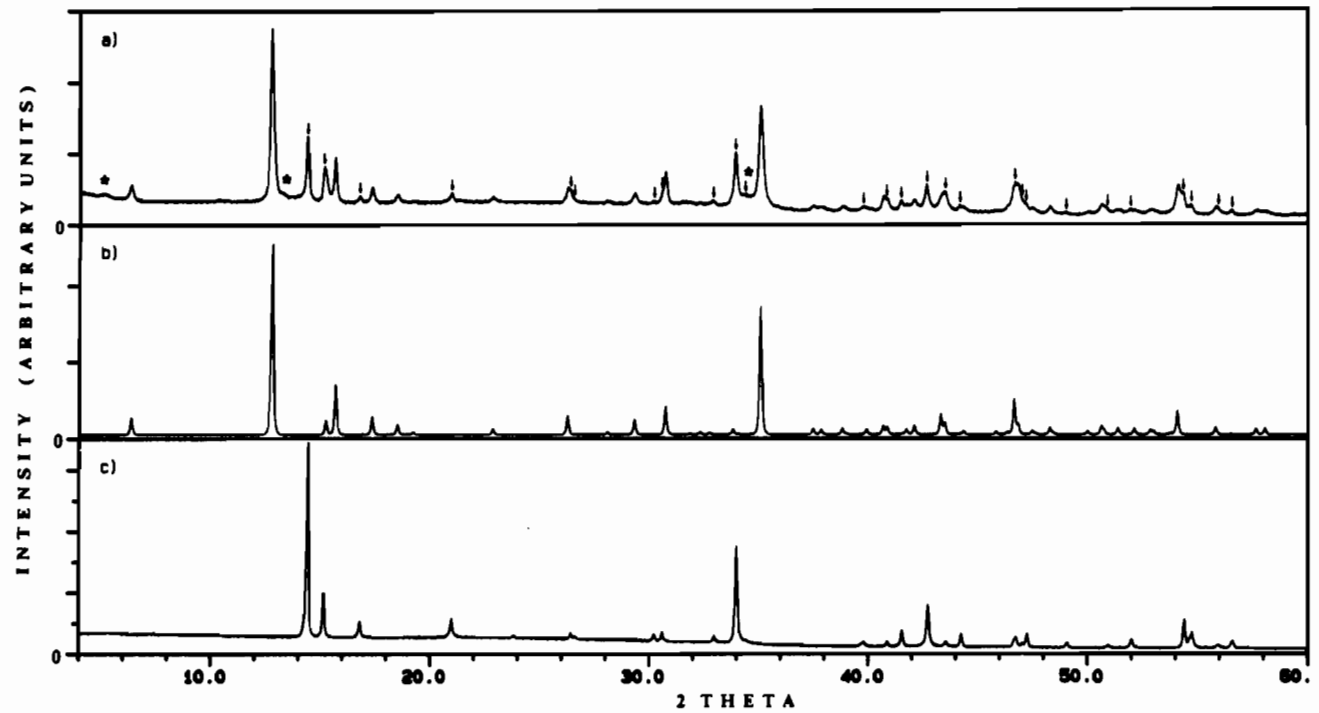

Figure 2. (a) Powder X-ray diffraction diagram of a 72.6% β'-$NaNb_3Cl_8$ + 27.4% α-Nb_3Cl_8 product mixture. Arrows indicate the α-Nb_3Cl_8 reflection positions; stars, the unidentified reflections. (b) Theoretical powder pattern calculated for β'-$NaNb_3Cl_8$ in $R\bar{3}m$ with the following approximate positional parameters: Na1 (special position 3a); Na2 (3b); Nb (18h), $x = 0.194$, $z = 0.078$; Cl1 (18h), $x = 0.831$, $z = 0.046$; Cl2 (18h), $x = 0.499$, $z = 0.119$; Cl3 (6c), $z = 0.111$; Cl4 (6c), $z = 0.368$. (c) Powder pattern of α-Nb_3Cl_8 starting material ($P\bar{3}m1$, $a = 6.744$ Å, $c = 12.268$ Å).[6,5c]

$Na_{0.732}Nb_3Cl_8$, which average to $Na_{0.726}Nb_3Cl_8$.

Methanol or water deintercalated $NaNb_3Cl_8$. For the water reaction, within a few seconds of addition of ~20 mL of distilled H_2O to ~50 mg of reaction product, gas evolution was noted. The H_2O was then allowed to evaporate to dryness in air. For the methanol reaction, again ~20 mL of methanol was added to ~50 mg of reaction product, under argon atmosphere, and in this case gas evolution was noted within a few minutes, increased in rate, and died off after several hours. The product was filtered out and dried in vacuo for ~1 day.

X-ray Investigation. Powder X-ray diffraction diagrams were obtained with a STOE automated powder diffraction system (STADE-P) or a modified Guinier technique[13] (Cu $K\alpha_1$ radiation) on samples loaded and sealed in 0.2-mm glass capillaries with silicon as external reference. A sample chemically analyzing as $Na_{0.726}Nb_3Cl_8$ appears from its powder X-ray diffraction pattern to be a mixture of unreacted α-Nb_3Cl_8 and a new product identified as $NaNb_3Cl_8$. From this diffraction pattern (Figure 2a) $NaNb_3Cl_8$ was indexed to an R-lattice with hexagonal cell constants $a = 6.774$ (1) Å and $c = 41.52$ (1) Å on the basis of the strongest 40 reflections that remained after those from α-Nb_3Cl_8 were removed. Three weak or very weak unidentified reflections at $2\theta = 5.15$, 13.22, and 34.65° were also noted. Several small crystals were examined on a Buerger precession X-ray camera and could be identified as either α-Nb_3Cl_8 or the new product $NaNb_3Cl_8$; however, they either were all twinned or showed broadened reflections.

The products from the deintercalation reactions were indexed and identified as α-Nb_3Cl_8; however, the reflections were somewhat broadened. Additionally, the product from the water reaction contained a small amount of NaCl, which most probably resulted from decomposition reactions.

Magnetic Measurements. Magnetic susceptibility data were recorded with the use of an SHE VTS SQUID susceptometer operating at a field flux density of 10 kG. The sample analyzing for $Na_{0.726}Nb_3Cl_8$ displayed a similar temperature dependence of the susceptibility as α-Nb_3Cl_8 but at reduced magnitudes. After subtraction of a 27.4% contribution from α-Nb_3Cl_8 to the susceptibility, $NaNb_3Cl_8$ showed a virtually temperature-independent paramagnetism with $\chi_M = 2 \times 10^{-4}$ emu/mol after correction for the core diamagnetic contribution.

Similar intercalation attempts on β-Nb_3Br_8 and β-Nb_3I_8 gave results different from those found for α-Nb_3Cl_8. β-Nb_3I_8 did not intercalate but instead underwent slow secondary reactions where NaI was observed in the powder patterns of the products. β-Nb_3Br_8 does apparently intercalate; however, the product occurs as a phase width "$Na_xNb_3Br_8$" ($x <$ 1.25 by wet chemical analysis) and NaBr was observed in some of the reaction products. This phase width can be indexed on a β-structure with maximum cell constants $a = 7.09$ Å and $c = 42.66$ Å (β-Nb_3Br_8: $a = 7.080$ Å, $c = 38.975$ Å).[5a] Additionally, the product disproportionates to β-Nb_3Br_8 and "$Na_yNb_3Br_8$" (R-lattice, $a = 7.09$ Å and $c = 43.48$ Å) upon heating of the solid at 120 °C for an extended time. Further studies are continuing to examine the exact nature of the reactions, the stoichiometries, and the structures and properties of these products.

Results and Discussion

The indexing of $NaNb_3Cl_8$ to an R-lattice with hexagonal cell constants $a = 6.774$ (1) Å and $c = 41.52$ (1) Å suggests the space group $R\bar{3}m$ when one notes that α-Nb_3Cl_8 is in $P\bar{3}m1$. Only three of the six possible stacking sequences allowed a close packing of anions (giving preferred octahedral vacancies over trigonal-prismatic vacancies), and these we have termed the γ-, β-, and β'-structure types (Figure 1). The very strong intensity of the 208 reflection vs the 027 reflection in the powder diagram clearly indicates a β'-structure for $NaNb_3Cl_8$. For a β- or γ-type structure 027 should be much stronger than 208. Therefore, the phase transition that occurs upon reduction and intercalation of α-Nb_3Cl_8 by sodium proceeds through a mechanism of M_3X_8 cluster layer shifts at all van der Waals gaps (α-h-anion lattice → β'-c-anion lattice). The powder diagram of a reaction product mixture of β'-$NaNb_3Cl_8$ and α-Nb_3Cl_8 is shown in Figure 2 along with a theoretical powder pattern calculated, by using only approximate positional parameters, and the powder pattern from the α-Nb_3Cl_8 starting material. The relative intensities of the theoretical pattern correlate fairly well. Only octahedral sites are large enough to accommodate the Na^+ ion due to its large ionic radius,[14] and occupying those sites within the A-gap (site III of Figures 1c and 3c) at (0, 0, 0) and the B-gap (site I of Figures 1c and 3c) at (0, 0, 0.5) gave the best fit to the powder pattern. Additionally, these are the octahedral sites found to be occupied in the crystal structures of the isotypic $LiZn_2Mo_3O_8$ and $Zn_3Mo_3O_8$. Diffusion of Na to site III at (0, 0, 0), in the A-gap (Figures 1c and 3c), and to site I at (0, 0, 0.5), located in the B-gap at the center point of two M_3 triangles oriented in a trigonal antiprism (Figures 1c and 3a), expands the c axis by 1.57 Å per two M_3X_8 cluster layers.

(13) Simon, A. *J. Appl. Crystallogr.* **1970**, *3*, 11.

(14) Shannon, R. D. *Acta Crystallogr.* **1976**, *A32*, 751.

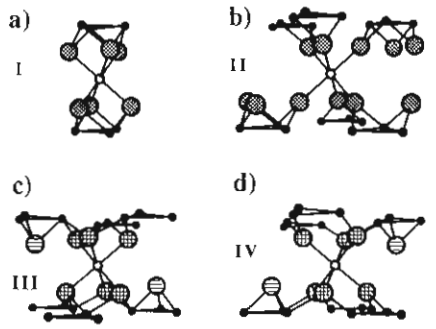

Figure 3. Perspective illustrations of the possible octahedral coordination sites of Na for the different phases highlighting the coordination of the respective halides (most unnecessary atoms removed for clarity): (a) B-layer, β'- and β-forms, X2-sp^3; (b) B-layer, α- and γ-forms, X2-sp^2; (c) A-layer, β'-, α'-, and γ-forms, X1-sp^3; (d) A-layer, α- and β-forms, X1-sp^2. The B-layer, α'-form is not represented, as this is a trigonal-prismatic site. See Figure 1 for atom representations.

The a-axis expansion is much smaller, being only 0.030 Å. The volume increase per Nb_3Cl_8 unit is 33.4 Å^3, which, according to Biltz's volume increment data,[15] corresponds to 3.1 Na^+ ions or 0.9 Na atom. It is remarkable that the volume increase corresponds closely to the atomic volume of Na despite a rather complete 3s orbital electron transfer into the cluster 4d orbitals.

The results from the magnetic measurements are in agreement with an $^1A_1$ electronic ground state expected from the theoretical picture[16] constructed for such M_3X_8 type cluster systems, which, for eight electron clusters, suggest the HOMO to be a filled a_1 orbital and the LUMO an e orbital. A simple visualization of these orbitals can be made by employing a right-handed Cartesian coordinate system on each Nb center with the X4–X3 axis representing the z axis, the x axis lying within the plane of the Nb_3 triangle, and the y axis taking its proper position. With this arrangement, the d_{xy}, d_{z^2}, p_x, p_y, p_z, and s metal orbitals are used to bond the six chlorides in the octahedral field and the remaining $d_{x^2-y^2}$, d_{xz}, and d_{yz} orbitals are responsible for metal–metal bonding. Applying simple group theory techniques on these orbitals to produce LCAO–MO's, one finds the molecular orbital ordering to be $1a_1$ (d_{yz}) < $1e$ (d_{xz}) < $2a_1$ ($d_{x^2-y^2}$) < $2e$ ($d_{x^2-y^2}$) < $3e$ (d_{yz}) < $1a_2$ (d_{xz}). This is exactly the ordering previously found,[16] but under this visualization both the $2a_1$ HOMO and 2e LUMO have primarily $d_{x^2-y^2}$ orbital metal contribution where the HOMO is a M–M bonding symmetry combination and the LUMO a M–M antibonding symmetry combination. Should the α-form have endured in $NaNb_3Cl_8$ (or a γ-type formed), the six X2 ligands of the B-gap forming site II (Figures 1b,d and 3b) and originating from six different clusters would have more sp^2-like character. The chloride p orbitals would now be well aligned for π overlap with the filled metal orbitals of the $2a_1$ HOMO as well as those of the 2e LUMO, the first being an unfavorable repulsive interaction and the latter destabilizing M–M and M–L antibonding interactions. This situation is alleviated by a transition to either the β- or β'-forms, where the change in sodium coordination to the six X2 ligands, now originating from only two clusters at site I (Figure 3a), allows them to remain essentially sp^3-like and the unfavorable M–L π interactions are largely removed. This result offers a dynamic example in support of Torardi and McCarley's[5b,7] suggestion that decreasing the M–L π interactions of these edge-bridging ligands is important to stabilize seven- and eight-electron M_3X_8 cluster derivatives. These authors argued that the M–X2 π interactions destabilize the $2a_1$ orbital to a M–M antibonding state (in six- and seven-electron derivatives) and for this reason longer M–M bond distances are observed in seven- and eight-electron $Mo_3O_8^{n-}$ derivatives when compared to six-electron derivatives. An alternate proposal from Bursten et al.[16c] suggested that the combined influence of a larger cluster metal effective ionic radius in the reduced species together with a shift of electron density, originating from ligand to metal σ-electron donation, from occupied M–M bonding symmetry orbitals into M–M antibonding symmetry orbitals in eight-electron derivatives causes the longer M–M bonds.

To investigate the preference of the β'-structure over the β-structure (both having the identical B-gap) in $NaNb_3Cl_8$, we performed MAPLE (Madelung part of the lattice energy) calculations,[17] based on point charge electrostatic nearest-neighbor interactions, on the β- and β'-models for $NaNb_3Cl_8$ as well as all five forms for Nb_3Cl_8. In the latter case, with the real α-Nb_3Cl_8 structure as the starting point, all energies (both total and positional) were found to be within 0.2% of one another and confirm the validity of the structural modeling procedure. This can be contrasted to the 1% difference in total lattice energy found between the β- and β'-models of $NaNb_3Cl_8$, where the β-structure was, in fact, slightly more stable (an effect of greater Nb–Na cation repulsions arising from the Na^+ found in the A-gap of the β'-phase). Moreover, the closer structural relationship between the α-form and the β-form would suggest that the β-form is kinetically more accessible. We can therefore argue that the β'-form prevails in $NaNb_3Cl_8$ due to a stabilizing effect of reduced M–X1 π interactions. Thus, the bonding of Na^+ in the A-gap at site IV (Figure 3d) at (0, 0, 0) of a β-type would cause a more sp^2-like state of the X1 orbitals. Similar to the X2 orbitals in the B-gap previously discussed, the p orbitals would also be well aligned for π interaction with both the filled $2a_1$ HOMO and the 2e LUMO.[18] The destabilization of the e LUMO (due to its M–M and M–L antibonding character) caused by these orbital interactions and the repulsion from the filled a_1 HOMO provides the driving force for the structural transition to the β'-form, where the ligands remain more sp^3-like (Figure 3c) and the long-pair orbitals are directed away from the Nb_3 triangles. These results clearly show the influence of the metal–X1 terminal ligand orbital interactions on the relative stability of eight-electron M_3X_8 cluster derivatives. VSEPR theory also suggests a reason for the structural variant found for $NaNb_3Cl_8$ (and likewise applicable to the $Mo_3O_8^{n-}$ compounds). Thus, in forming the β'-type, one of the lone electron pairs on each of the six surrounding chlorides of the octahedral sites I and III is directed toward the sodium cation (Figure 3). The other forms either would not allow this directed interaction or would require the cation to occupy a tetrahedral site in either the A- and/or the B-layers.

The above discussions suggest that the a_1 HOMO has considerable M–L antibonding character and this has a strong effect on the structure. This means that the longer M–M bond distances observed in the seven- and eight-electron derivatives of certain M_3X_8 type clusters over the corresponding six-electron derivatives may not be due to electron population of M–M antibonding orbitals. Thus, the increased electron densities in M–L antibonding states in the seven- and eight-electron derivatives lengthen the M–L bond distances and, so as to optimize the geometrical arrangement for favorable M–L bonding orbital overlaps, induce longer M–M bond distances. Certainly, this ligand matrix influence can be seen when one compares the M–M bond distances found in molecular clusters to those found in corresponding polymeric clusters: $[Mo_3O_4(C_2O_4)_3(H_2O)_3]^{2-}$[19] (2.486 Å, six electrons, molecular), $Zn_2Mo_3O_8$[5f] (2.524 Å, six electrons, polymeric); $[Mo_3OCl_3(O_2CCH_3)_3(H_2O)_3]^{2+}$[20] (2.550 Å, eight electrons, molecular), $Zn_3Mo_3O_8$[5b] (2.580 Å, eight electrons, polymeric), $LiZn_2Mo_3O_8$[5b] (2.578 Å, seven electrons, polymeric). In all cases, the molecular

(15) Biltz, W. *Raumchemie der festen Stoffe*; Leopold Voss Verlag: Leipzig, 1934.
(16) (a) Cotton, F. A. *Inorg. Chem.* **1964**, *3*, 1217. (b) Bullett, D. W. *Ibid* **1980**, *19*, 1780. (c) Bursten, B. E.; Cotton, F. A.; Hall, M. B.; Najjar, R. C. *Ibid* **1982**, *21*, 302. (c) Müller, A.; Jostes, R.; Cotton, F. A. *Angew. Chem.* **1980**, *92*, 921.
(17) A full discussion of the MAPLE calculations and their applications and limitations can be found in: Hoppe, R. *Adv. Fluorine Chem.* **1970**, *6*, 387. Hoppe, R. *Angew. Chem.* **1966**, *78*, 52. Hoppe, R. *Angew. Chem., Int. Ed. Engl.* **1966**, *5*, 95.
(18) The higher energy levels of the terminal chlorides offer a better energy overlap with the metal orbitals of the e LUMO than do those of the bridging chlorides.
(19) Bino, A.; Cotton, F. A.; Dori, Z. *J. Am. Chem. Soc.* **1978**, *100*, 5252.
(20) Bino, A.; Cotton, F. A.; Dori, Z. *Inorg. Chim. Acta* **1979**, L133.

cluster, which has the greater freedom in ligand orientation, maintains the shorter M–M bond distance. Especially noteworthy is the latter comparison where even the presence of chloride ligands at the X2 positions of the eight-electron molecular cluster do not induce longer M–M distances than those found in the all-oxide seven-electron polymeric cluster. Additionally, the question of the M–M bonding or antibonding character of the $2a_1$ orbital seems clear, at least in the case of the niobium chloride clusters, where it has been noted that in the six-electron $[Nb_3Cl_{10}(P(C_2H_5)_3)_3]^{-}$[21] molecular cluster the Nb–Nb bond distances (2.976 Å) are considerably longer than those found in either the eight-electron molecular cluster $Nb_3Cl_7(P(CH_3)(C_6H_5)_2)_6$[22] (2.832 Å) or the seven-electron polymeric clusters in α-Nb_3Cl_8 (2.81 Å). The slightly longer distances found in $Nb_3Cl_7(P(CH_3)(C_6H_5)_2)_6$ compared to α-Nb_3Cl_8 may be due to the weak π-acceptor ability of the phosphine ligands.

When sodium intercalates into α-Nb_3Cl_8, only β'-$NaNb_3Cl_8$ is formed, with no phase width or interim phases being observed in the powder pattern. Even when a deficiency of sodium is used, only a mixture of β'-$NaNb_3Cl_8$ and α-Nb_3Cl_8 is observed as product. It may therefore be concluded that the rate-determining step occurs within the initial surface reduction reaction step(s). The apparent high diffusion rate of Na within the lattice is aided by the requirement to form the β'-structure, where cluster layers must shift relative to one another at all van der Waals gaps. This is supported by the observation that the re-formation of α-Nb_3Cl_8 from the deintercalation of β'-$NaNb_3Cl_8$, through the reduction of water or methanol, likewise occurs over several hours and begins within minutes of exposure.

Synthetic procedures for Nb_3Cl_8 employ temperatures of ~800 °C, and the α-phase is the only phase formed.[5a] Synthetic attempts at preparing $NaNb_3Cl_8$ from mixtures of α-Nb_3Cl_8, Nb, and NaCl in sealed ampules at temperatures of 800–1050 °C gave only α-Nb_3Cl_8, Nb_6Cl_{14}, $NaNb_6Cl_{15}$, and/or $Na_4Nb_6Cl_{18}$ as products.[23] The reversible nature of the α-Nb_3Cl_8/β'-$NaNb_3Cl_8$ system further illustrates that the α-form of Nb_3Cl_8 is the most stable (in contrast to Nb_3Br_8 and Nb_3I_8, which are reported to form both α- and β-phases).[5a] When sodium deintercalates from β'-$NaNb_3Cl_8$ at room temperature, if the lattice were to simply contract as the β'-form, the six lone-pair orbitals of the X2 ligands in the B-gap previously directed toward Na^+ (Figure 3a) would continue to point toward one another and would come very close at the 2.969-Å spacing of these anions in Nb_3Cl_8. These orbitals thus repel each other and drive the structural transition back to the α-form, where they now point toward an X3 ligand of a tetrahedral site at a spacing of 3.276 Å. Although the structural relationship of the β'-form to the α'-form is closer than that to the α-form (mechanistic considerations), the non-close-packing of anions at the B-gap of an α'-type (i.e. a trigonal-prismatic site) brings these X2 orbitals in even closer contact than in a β'-structure. Thus, the α'-, β'-, and β-forms all require larger cell dimensions than those achieved in the α-form, and for this reason Nb_3Cl_8 exists with the α-structure. An increased polarizability of the lone-pair orbitals should stabilize the β- or β'-structures in this respect, as is observed for β-Nb_3Br_8 and β-Nb_3I_8.[5a]

The X-ray pattern of β'-$NaNb_3Cl_8$ is observed (with small changes occurring at ~100 and ~200 °C) up to ~400 °C, at which point the phase loses some or all of the Na in the form of NaCl. Intriguingly, the powder diagram of the product closely resembles the theoretical diagram expected for a γ-Nb_3Cl_8 phase. These investigations are continuing.

Conclusions

We have reported here the first characterized unsolvated intercalation product from a binary metal halide with a very electropositive alkali metal. It is surprising to find this reaction with an early-transition-metal compound. It was shown that $NaNb_3Cl_8$ could form either a β- or β'-structure in order to reduce edge-bridging (X2) M–L π interactions and provide for directed lone pair to cation interactions in the B-gap. So as to reduce terminal (X1) M–L orbital interactions and likewise give directed lone pair to cation interactions in the A-gap, the β'-structure is formed. Thus, a structural transition ensues whereby all Nb_3Cl_8 cluster layers must shift relative to one another at all van der Waals gaps, and this enhances ion diffusion. These results, discussed in connection with results for other $M_3X_8^{n-}$ cluster derivatives, seem to indicate that M–L antibonding orbital interactions have a strong influence on M–M bond distances within the cluster triangles. The α-phase is the stable form for Nb_3Cl_8 because other related forms cause much too close contacts between directional long-pair orbitals of the edge-bridging (X2) atoms.

Acknowledgment. We gratefully acknowledge the help of Dr. R. K. Kremer (magnetic measurements), Dr. J. Köhler (MAPLE calculations and powder X-ray diffractometer measurements), and W. Röthenbach (Guinier photographs) and thank Prof. R. Hoppe for the use of his MAPLE program.

(21) Cotton, F. A.; Diebold, M. P.; Roth, W. J. *J. Am. Chem. Soc.* **1987**, *109*, 2833.
(22) Cotton, F. A.; Kibala, P. A.; Roth, W. J. *J. Am. Chem. Soc.* **1988**, *110*, 298.
(23) Sägebarth, M. Dissertation, Universität Stuttgart, 1989.

Contribution from the Laboratoire de Chimie du Solide et Inorganique Moléculaire, URA CNRS 254, Université de Rennes I, 35042 Rennes Cedex, France

The Possible Existence of a Heteronuclear Octahedral Hypercloso Cluster: Can N_2 or an Alkyne Be Complexed through a M_4L_n Square?

Samia Kahlal, Jean-François Halet,* and Jean-Yves Saillard*

Received November 19, 1990

In previous theoretical studies, we have rationalized the electronic structure of a class of octahedral organometallic clusters of general formula $L_nM_4E_2$, shown in **1**, where M is a transition

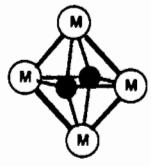

1

metal and E (black dot in **1**) is a main-group atom or a conical fragment from the third and fourth period, such as S, Se, PR, GeR, ...[1] The total valence electron count adopted by these closo clusters is either 66 electrons, i.e. seven skeletal electron pairs (SEP's) or 68 electrons (eight SEP's). The 66-electron count satisfies the polyhedral skeletal electron pair theory (PSEP),[2] while the 68-electron count corresponds to the occupation of an extra skeletal MO, which is weakly π-antibonding between the metal atoms.[1] In these clusters, because of the difference in the covalent radii of M and E, and consequently because of the difference in M–M and M–E bond lengths, the two E atoms capping the metallic square are forced to be rather close to each other (the E···E distance is about 20% longer than the one expected for a single bond). We have shown that such a short E···E contact can exist only because the corresponding electronic interaction is significantly bonding, whatever is the cluster electron count (seven or eight SEP's).

(1) (a) Halet, J.-F.; Hoffmann, R.; Saillard, J.-Y. *Inorg. Chem.* **1985**, *24*, 1695. (b) Halet, J.-F.; Saillard, J.-Y. *New J. Chem.* **1987**, *11*, 315. (c) Albright, T. A.; Yee, K. A.; Saillard, J.-Y.; Kahlal, S.; Halet, J.-F.; Leigh, J. S.; Whitmire, K. H. *Inorg. Chem.* **1991**, *30*, 1179.
(2) (a) Wade, K. *J. Chem. Soc., Chem. Commun.* **1971**, 792. (b) Mingos, D. M. P. *Nature (London) Phys. Sci.* **1972**, *236*, 99. (c) Wade, K. *Adv. Inorg. Chem. Radiochem.* **1976**, *18*, 1. (d) Wade, K. In *Transition Metal Clusters*; Johnson, B. F. G., Ed.; Wiley and Sons: New York, 1980, p 193. (e) Mingos, D. M. P. *Acc. Chem. Res.* **1984**, *17*, 311.

0020-1669/91/1330-2567$02.50/0